RESEARCH ARTICLE

SAMRIDDHI Volume 13, Issue 2, 2021 Print ISSN : 2229-7111 Online ISSN : 2454-5767

Normal Mode Analysis, Electronic Descriptors, NLO Properties & Molecular Docking of "Butein, 2',3,4,4'-Tetrahydroxychalcone: A DFT approach"

Tanveer Hasan*[1], Syed Hasan Mehdi[2], Syed Shabihe Raza Baqri[3], P. K. Singh[4]

1.* Department of Physics, Shia Post Graduate College, Lucknow, India; e-mail : tanveerhasan09@gmail.com
2. Department of Chemistry, Shia Post Graduate College, Lucknow, India.
3. Department of Zoology, Shia Post Graduate College, Lucknow, India.
4. Department of Humanities & Applied Sciences, School of Management Sciences, Lucknow, India.

ABSTRACT

Study of modern medicine is a flourishing field with activity revolving around the identification, characterization and assessment of therapeutic potential of phytochemicals in various disease conditions. Chalconoids, being prominently present in various medicinal herbs are being widely studied to unravel the molecular mechanisms associated with their effects. This paper describes the molecular structure of well known compound "(Butein, 2',3,4,4'-Tetrahydroxychalcone [$C_{15}H_{12}O_5$]", which has been optimized and its structural parameters have been calculated by DFT/B3LYP method using 6-311++G(d,p) basis set. The fundamental vibrational wavenumbers and their intensities were calculated and a good agreement between the observed FTIR spectrum and scaled calculated wavenumbers has been achieved. The electronic properties of the compound are explained using HOMO-LUMO and MEPS descriptors. The Non-Linear Optical parameters (NLO) are discussed using electrical parameters like electric dipole moment, molecular polarizability and hyperpolarizability measurements. We have done the molecular docking analysis also, in order to get a better perception into its observed physiological effects which are a prerequisite for determining its therapeutic potential. We hereby report a strong interaction of butein with the protein 1OG6, an enzyme of cytochrome P450 series designated CYP2C9 which is intricately involved in oxidative metabolic pathways. This provides a plausible mechanism for anti-oxidant properties of butein.

Keywords: Butein (2', 3, 4, 4'-Tetrahydroxychalcone) [$C_{15}H_{12}O_5$]; DFT, Vibrational Assignments, Enzyme cytochrome P450, NLO parameters, Molecular Docking.

SAMRIDDHI : A Journal of Physical Sciences, Engineering and Technology, (2021); DOI : 10.18090/samriddhi.v13i02.12

INTRODUCTION

Traditional herbs have been profusely described in ancient medical literature sourced from diverse cultures of the world. Although the medicinal properties of a great majority of herbs have been proven in random studies yet the exact mechanisms of their action remain unknown in most cases. The availability of sophisticated techniques in analytical chemistry today has led to a gush of growth in exploration of active principles present in medicinal plants. Chalcones, also known as benzyl acetophenone or benzylideneacetophenone are very important intermediate for the synthesis of various biological active compounds. They themselves possess a broad spectrum of biological activities like antibacterial, antioxidative, antiviral, antiulcer, anticancer etc. [1]. Chalcones are precursor compounds

Corresponding Author : Tanveer Hasan, Department of Physics, Shia Post Graduate College, Lucknow, India; e-mail : tanveerhasan09@gmail.com

How to cite this article : Hasan, T., Mehdi, S.H., Baqri, S.S.R., Singh, P.K. (2021). Normal Mode Analysis, Electronic Descriptors, NLO Properties & Molecular Docking of "Butein, 2',3,4,4'-Tetrahydroxychalcone: A DFT approach."

SAMRIDDHI : A Journal of Physical Sciences, Engineering and Technology, Volume 13, Issue (2), 135-146.

Source of support : Nil

Conflict of interest : None

for flavonoid synthesis in plants, and they can also be synthesized in laboratory. Butein, a chalcone compound belonging to the flavonoid subclass is abundantly present in plants such as *Buteamonosperma* and *Toxicodendronvernicifluum* etc. and is known to possess several medicinal properties [2(a)]. For instance, it is reported to be an effective antioxidant that possibly works by hydrogen atom transfer mechanism and metal chelate mechanism [2(b)]. The free radical lurking and metal ion chelation activity of butein protects cells against the peroxidation of lipids for instance the plasma membrane and of low-density lipoprotein (LDL) [3]. Considering the critical role played by lipid peroxidation in mechanisms of cellular senescence, butein can be employed in conditions that involve aging effects. Besides, *Rhusverniciflua* Stokes (RVS) has been used as a traditional herbal medicine for its antiadipogenic effects to overcome obesity. Carefully separation led to the identification of anti-adipogenic functions of butein [4]. Recent research shows the inhibitory effects of butein on lipid metabolism in *Caenorhabditiselegans*[5].In other research butein is reported to be an aromatase inhibitor with great potential to be exploited as a natural alternative for the chemoprevention of breast cancer [6]. Butein, which is atetrahydroxychalcone, is reported to exhibit the anti-inflammatory effects, with its action mechanisms using TNF-α-stimulated keratinocytes. Butein significantly inhibited TNF-α-induced ICAM-I expression and monocyte adhesion in human keratinocyte cell line HaCaT [7]. Butein is implicated in aldose reductase activity which controls the reduction of aldose and converts glucose into sorbitol thereby facilitating the formation of fructose from glucose [8].

The present study produces some theoretical quantum chemical calculations of the “Butein (2',3,4,4'-Tetrahydroxychalcone)” by DFT/B3LYP method using 6-311++G(d,p) as basis set. The equilibrium structure of butein is obtained and intra-molecular interaction is discussed by quantum theory of atoms in molecule (QTAIM). The calculated spectrum has been compared with the experimental FT-IR spectrum. The electronic descriptors like HOMO, LUMO, energy band gap and molecular electrostatic potential surface (MEPS) analyses along with calculation of some electrical parameters like dipole moment, molecular polarizability and first static hyperpolarizability, are used to predict the NLO properties of the molecule. Since the present compound possesses some biological activities which are of medicinal importance we have also performed molecular docking study of the compound to get a deeper insight into its possible target molecules. Among the many possible candidates for docking studies, the molecules involved in oxidative metabolism figure prominently because of anti-oxidant properties of butein. The other contenders for its targets are molecules from bacterial cell surface which may impart antibiotic activity to butein. In this study, we narrowed down on molecules involved in oxidative metabolism and found a tight docking of butein with the protein 1OG6 which is obtained from protein database bank. This protein is a liver monooxygenase of cytochrome P450 series designated CYP2C9 which is involved in NADPH-dependent electron transport pathway to oxidize a variety of xenobiotics in liver microsomes. This observation fits well with the predicted anti-oxidant properties of butein. However, there is still a possibility that butein may interact more strongly with certain other biomolecules that would explain its other physiological effects.

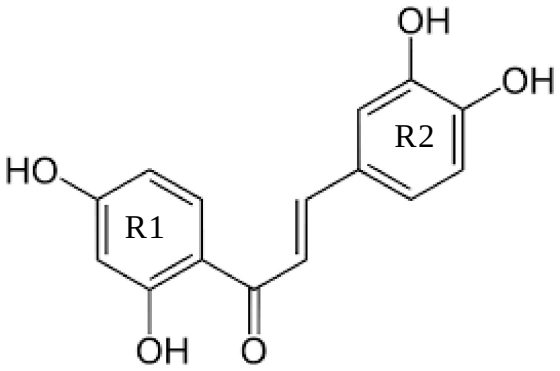

Figure 1 (a) : Molecular structure of butein

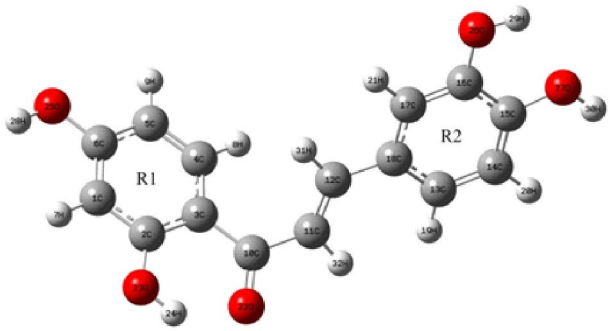

Figure 1 (b) : Model molecular structure of butein 2', 3, 4, 4'-Tetrahydroxychalcone

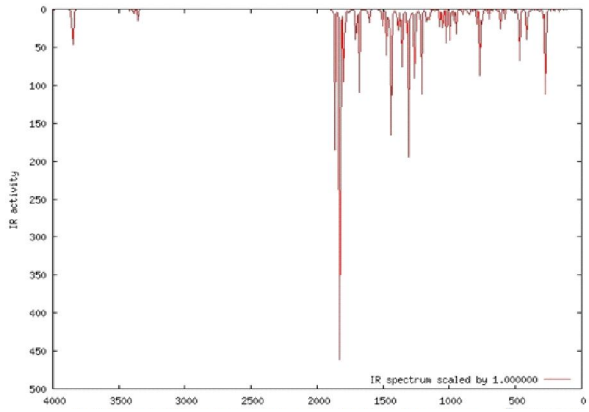

Figure 2: Theoretical IR spectra of butein as plotted by GaussSum software Frequency cm-1

COMPUTATIONAL METHODS

Entire calculations have been performed using of Gaussian 09 software, entreating gradient geometry optimization and utilizing the B3LYP/6-311++G (d,p) levels of theory to obtain the molecular structure and vibrational wave numbers [9,10].This basis set 6-311G (d, p), with 'p' polarization functions on hydrogen atoms and 'd' polarization functions on heavy atoms, is used for better description of polar bonds of molecule [11,12]Initial geometry is modelled with the help of Gaussview software 5.0.8.2 and the model molecular structure is shown in figure 1(b) [13].The molecular geometry is fully optimized by Becke's three parameter exchange term combined with the gradient-corrected correlation functional of Lee, Yang and Parr [14-16]. The potential energy distribution (PED) analysis has been performed by VEDA 4 software [17]. The spectral values of butein have been taken from the reported literature and its theoretically calculated IR spectrum with Gauss Sum software is presented in figure 2 [18(a), 18 (b)].

RESULT AND DISCUSSION

The vibrational wave numbers are calculated from the optimized structural parameters. No negative vibrational wave numbers were appeared in the calculated values which, ensures the minimum energy of the conformer.

Optimized Molecular Geometry

The optimized structural parameters calculated by B3LYP at 6-311++G (d, p) basis set are provided in supplementary Table T-I.

Table TI : Optimized ground state structural parameters of butein at B3LYP method

S.No.	Parameters	Method
	Stretching	**DFT**
	Angstrom	**B3LYP**
1	C1-C2	1.38
2	C1-C6	1.37
3	C1-H7	1.07
4	C2-C3	1.4
5	C2-O23	1.35
6	C3-C4	1.4
7	C3-C10	1.47
8	C4-C5	1.37
9	C4-H8	1.07
10	C5-C6	1.39
11	C5-H9	1.07
12	C6-O25	1.36
13	C10-C11	1.48
14	C10=O22	1.24
15	C10-H32	2.13
16	C11=C12	1.33
17	C11-H19	2.78
18	C11-H32	1.07
19	C12-C18	1.47
20	C12-H31	1.07
21	C13-C14	1.38
22	C13-H18	1.39

S.No.	Parameters	Method
	Stretching	**DFT**
	Angstrom	**B3LYP**
86	C2-O23-O22	85
87	C2-O23-H24	113
88	O22-O23-H24	29
89	C6-O25-H28	115
90	C16-O26-H29	113
91	C15-O27-H30	115
	Dihedral Angles(deg)	
92	(C6,C1,C2,C3)	2.07
93	(C6,C1,C2,O23)	-178.55
94	(H7,C1,C2,C3)	-178.97
95	(H7,C1,C2,O23)	0.41
96	(C2,C1,C6,C5)	0.35
97	(C2,C1,C6,O25)	179.50
98	(H7,C1,C6,C5)	-178.57
99	(H7,C1,C6,O25)	0.58
100	(C1,C2,C3,C4)	-3.29
101	(C1,C2,C3,C10)	178.67
102	(O23,C2,C3,C4)	177.38
103	(O23,C2,C3,C10)	-0.66
104	(C1,C2,O23,O22)	173.98
105	(C1,C2,O23,H24)	171.55
106	(C3,C2,O23O22)	-6.66

S.No.	Parameters	Method
	Stretching	DFT
	Angstrom	B3LYP
23	C13-H19	1.07
24	C14-C15	1.38
25	C14-H20	1.07
26	C15-C16	1.39
27	C15-O27	1.38
28	C16-C17	1.37
29	C16-O26	1.37
30	C17-C18	1.39
31	C17-H21	1.07
32	H21-O26	2.56
33	O22-O23	2.61
34	O22-H24	1.84
35	O23-H24	0.95
36	O25-H28	0.96
37	O26-H29	0.95
38	O27-H30	0.94
39	C2-C1-C6	120
40	C2-C1-H7	118
41	C6-C1-H7	122
42	C1-C2-C3	121
43	C1-C2-O23	116
44	C3-C2-O23	123
45	C2-C4-C4	117
46	C2-C3-C10	120
47	C4-C3-C10	123
48	C3-C4-C5	122
49	C3-C4-H8	119
50	C5-C4-H8	119
51	C4-C5-C6	119
52	C4-C5-H9	122
53	C6-C5-H9	119
54	C1-C6-C5	121
55	C1-C6-O25	122
56	C5-C6-O25	117
57	C3-10-C11	123
58	C3-C10=O22	120
59	C11-C10=O22	117
60	C10-C11=C12	125
61	C10-C11-H32	112
62	C12-C11-H32	122
63	C11-C12-H31	119
64	C18-C12-H31	114
65	C11=C12-C18	127
66	C14-C13-C18	121
67	C14-C13-H19	119
68	C18-C13-H19	121
69	C13-C14-C15	120
70	C13-C14-H20	120
71	C15-C14-H20	120
72	C14-C15-C16	120
73	C14-C15-O27	125
74	C16-C15-027	115

S.No.	Parameters	Method
	Stretching	DFT
	Angstrom	B3LYP
107	(C3,C2,O23,H24)	-9.08
108	(C2,C3,C4,C5)	2.24
109	(C2,C3,C4,H8)	-176.24
110	(C10,C3,C4,C5)	-179.79
111	(C10,C3,C4,H8)	1.74
112	(C2,C3,C10,C11)	-161.40
113	(C2,C3,C10,O22)	17.82
114	(C4,C3,C10,C11)	20.67
115	(C4,C3,C10,O22)	-160.11
116	(C3,C4,C5,C6)	0.07
117	(C3,C4,C5,H9)	-179.42
118	(H8,C4,C5,C6)	178.55
119	(H8,C4,C5,H9)	-0.94
120	(C4,C5,C6,C1)	-1.41
121	(C4,C5,C6,O25)	179.39
122	(H9,C5,C6,C1)	178.09
123	(H9,C5,C6,C5)	-1.11
124	(C1,C6,O25,H28)	0.33
125	(C5,C6,O25,H28)	179.51
126	(C3,C10,C11,C12)	36.50
127	(C3,C10,C11,H32)	-151.38
128	(O22,C10,C11,C12)	-142.74
129	(O22,C10,C11,H32)	29.38
130	(C3,C10,O22,O23)	-16.21
131	(C11,C10,O22,O23)	163.05
132	(C10,C11,C12,C18)	174.30
133	(C10,C11,C12,H31)	-3.89
134	(H32,C11,C12,C18)	2.86
135	(H32,C11,C12,H31)	-175.34
136	(C11,C12,C18,C13)	4.40
137	(C11,C12,C18,C17)	-175.94
138	(H31,C12,C18,C13)	-177.34
139	(H31,C12,C18,C17)	2.33
140	(C18,C13,C14,C15)	-0.04
141	(C18,C13,C14,H20)	-180.00
142	(H19,C13,C14,C15)	179.90
143	(H19,C13,C14,H20)	-0.06
144	(C14,C13,C18,C12)	179.82
145	(C14,C13,C18,C17)	0.15
146	(H19,C13,C18,C12)	-0.12
147	(H19,C13,C18,C17)	-179.79
148	(C13,C14,C15,C16)	-0.06
149	(C13,C14,C15,O27)	-179.95
150	(H20,C14,C15,C16)	179.90
151	(H20,C14,C15,O27)	0.01
152	(C14,C15,C16,C17)	0.05
153	(C14,C15,C16,O26)	-179.89
154	(O27,C15,C16,C17)	179.95
155	(O27,C15,C16,O26)	0.01
156	(C14,C15,O27,H30)	-0.82
157	(C16,C15,O27,H30)	179.28
158	(C15,C16,C17,C18)	0.07

Table-1 cont ..

S.No.	Parameters	Method
	Stretching	DFT
	Angstrom	B3LYP
75	C15-C16-C17	120
76	C15-C16-O26	121
77	C17-C16-O26	119
78	C16-C17-C18	121
79	C16-C17-H21	118
80	C18-C17-H21	121
81	C12-C18-C13	123
82	C12-C18-C17	118
83	C13-C18-C17	119
84	C10-O22-O23	89
85	C2-O23-O22	84

S.No.	Parameters	Method
	Stretching	DFT
	Angstrom	B3LYP
159	(C15,C16,C17,H21)	179.91
160	(O26,C16,C17,C18)	-180.00
161	(O26,C16,C17,H21)	-0.15
162	(C15,C16,O26,H29)	-0.32
163	(C17,C16,O26,H29)	179.75
164	(C16,C17,C18,C12)	-179.85
165	(C16,C17,C18,C13)	-0.17
166	(H21,C17,C18,C12)	0.31
167	(H21,C17,C18,C13)	180.00
168	(C10,C2C2,O23,C2)	14.13

The presence of four hetero oxygen atoms$O_{23}O_{22}$ &$O_{26}O_{27,}$ led two available coordination sites in Butein, one is at the position of $O_{23}O_{22}$, and another is at the position of $O_{26}O_{27}$ (Figure. 1). The pair of oxygen atoms$O_{26}O_{27}$of one molecule may interact with H_{21}atom of another molecule and $O_{23}O_{22}$ of one molecule may interact with H_{32} atom of another molecule with H_{21}-O_{26}& H_{32}-O_{22}bond distances of 2.56and 2.13 Å respectively, which correspond with bifurcated H21& H32dihedral angles calculated as 179,-0.15°& 2.86, -175.86° , respectively. There is also possibility of hydrogen bonding at the atom position C_{11}-H_{19} suggested by the bond length calculated as 2.78 Å.

The optimized bond length of (C-C) in the six-member ring R1 ranges between 1.37- 1.40 Å, whereas in the ring R2, it is slightly greater and varies in the range of 1.37-1.47 Å. The optimized bond length of double bonding of (C10=O22) attached to ring R1 is calculated at 1.24 Å, which is as expected lesser than the single bonding (C2-O23), (C6-O25), (C15-O27) and (C16-O26) bond lengths calculated in the range 1.35-1.38 Å. The bond lengths of (C-H) and (O-H) are calculated as 1.07 &0.95 Å respectively.

Vibrational Analysis

The maximum number of potentially active observable fundamentals of a nonlinear molecule containing N-atoms is equal to (3N-6) [19].The title compound contains 32 atoms and hence exhibits 90 normal modes of vibratio1ns. The assignments of the calculated frequency are supported by and based on the animation of Gauss View 5.0.8, which gives a 3D-animated view of the vibrational modes. The potential energy distribution (PED) is calculated by VEDA 4 software program. To correct overestimations at the calculated harmonic frequencies an empirical uniform scaling factor of 0.983 up to 1700 cm^{-1} and 0.958 for above 1700 cm^{-1} were used [20].All the vibrational assignments are presented in supplementary Table T-II.

Table TII : Frequency assignments for BUTEIN at B3LYP/6-311G(d,p) in cm^{-1}, with PED % in Square Brackets

	Calc Freq		Exp Freq*	Assignment Modes[PED]
S.No.	Unscaled	Scaled	FTIR	
1	4061	3890	36101(w)	ν(O27-H30)[100]
2	4040	3870		ν(O25-H28)[100]
3	4013	3844		ν(O26-H29)[100]
4	3851	3689	3490 (w)	ν(O23-H24)[100]
5	3423	3279	3350(m)	ν(C5-H9)[66] + ν(C4-H8)[33] ***{Char}***
6	3404	3261		ν_s(C4-H8)[55] + ν_a(C5-H9)[28] + ν_a(C13-H19)[14]
7	3403	3261		ν_s(C4-H8)[11] + ν_s(C11-H32)[11]+ ν_s(C13-H19)[68]
8	3394	3252	2950(wsh)	ν_s(C17-H21)[98]
9	3394	3251	2870wsh)	ν_s(C1-H7)[99]
10	3382	3240		ν_s(C11-H32)[85] + ν_a(C13-H19)[11]

Table-II cont..

11	3360	3219		ν_s(C14-H20)[92]
12	3353	3212	2810(wsh)	ν_s(C12-H31)[98]
13	1868	1789	1820(wsh)	ν_s(C11=C12)[54]+ φ(H31-C12-C11)[10]a
14	1829	1752		ν_s(C16=C17)[27]+ ν_s(C13=C14)[11]
15	1827	1751		ν_s(C4=C5)[10]+ ν_s(C1=C2)[26]
16	1802	1727	1670(vs)	ν_s(O22=C10)[34]+ν_a(C6=C5)[15] ***{Char}***
				ν_a(C13=C18)[15]+ φ(C17-C16-C15)[14]
17	1792	1716	1630(s)	ν_s(O22=C10)[23]+ν_s(C6=C5)[16]+ν_a(C6=C5)[11]
18	1760	1686	1610(vs)	ν_s(C14=C15)[18]+ ν_a(C16=C15)[10] ***{Char}***
19	1705	1633	1535(s)	φ(H20-C14-C15)[22]+ φ(H19-C13-C14)[11]+φ(H21-C17-C18)[12]a
20	1684	1655		φ(H7-C1-C6)[16]+φ(H8-C4-C5)[20]+φ(H9-C5-C6)[12]
	1622	1595		φ(H18-C13-C14)[14]+φ(H29-O26-C16)[19]a+φ(H19-C13-C14)[14]
22	1606	1579		ν_a(O22=C10)[12]+ν_s(C4=C5)[11]+φ(H9-C5-C6)[17]
23	1510	1484		φ(H31-C12-C11)[27]+φ(H24-O23-C2)[16]
24	1504	1479		φ(H31-C12-C11)[25]a+φ(H24-O23-C2)[18]
25	1476	1451	1470(w)	ν_s(O23-C2)[12]+ν_s(O25-C6)[13]
26	1472	1447		φ(H32-C11-C12)[12]+φ(H31-C12-C11)[18]+
				φ(H19-C13-C14)[15] +φ(H21-C17-C18)[20]
27	1462	1437		φ(H32-C11-C12)[24]
28	1445	1421		ν_a(C4-C5)[11]+ ν_s(C14-C15)[10]+ν_a(C3-C10)[12]
29	1436	1412		ν_a(O26-C16)[11]+ν_a(C12-C18)[10]+φ(H32-C11-C12)[22]
30	1398	1374	1360(m)	ν_s(O27-C15)[22]+φ(H30-O27-C15)[10]
31	1389	1365		ν_s(C3-C4)[31]+φ(H7-C1-C6)[12]
32	1369	1346		ν_s(C13-C18)[13]
33	1356	1333		ν_a(C1-C2)[18]+φ(H24-C23-C2)[15]a+φ(H8-C4-C5)[10]a
34	1320	1298	1290(w)	ν_s(C16-C17)[15]+φ(H29-O26-C16)[26]a+
				φ(H19-C13-C14)[14] +φ(H20-C14-C15)[17]a
35	1306	1284		ν_s(C4-C5)[10]+ν_a(C1-C2)[11]+ν_s(O23-C2)[15]+
				ν_a(O25-C6)[14]+φ(H24-O23-C2)[10]a+φ(H7-C1-C6)[24]
36	1295	1273	1265(wsh)	ν_s(C13-C14)[16]+ν_a(C12-C16)[11]+
				φ(H30-O27-C15)[14]a+φ(H21-O17-C18)[24]
37	1264	1243	1240(vs)	ν_a(C4-C5)[15]+φ(H28-O25-C6)[18]+φ(H7-C1-C6)[26] ***{Char}***
38	1261	1240		ν_a(C1-C5)[13]+φ(H28-O25-C6)[36]+φ(H7-C1-C6)[10]a
39	1257	1236		ν_a(C16-C17)[13]+ν_a(C13-C14)[16]+φ(H7-C1-C6)[10]a+φ(H30-O27-C15)[14]
40	1212	1192	1190(vs)	φ(H30-O27-C15)[28]a+φ(C15-C14-C13)[16]+
				φ(C17-C16-C15)[11]+φ(C14-C15-C16)[11]
41	1173	1153		ν_a(C10-C11)[16]+φ(C5-C4-C3)[19]+τ(H31-C12-C18-C13)11]
42	1165	1145	1155(w)	τ(H8-C4-C5-C6)[43] + τ(H9-C5-C6-C1)[15]a
43	1151	1132	1120(w)	τ(H8-C4-C5-C6)[12]a + τ(H31-C12-C18-C13)[46]
44	1109	1090		τ(H19-C13-C18-C13)[45]a+τ(H20-C14-C15-C16)[32]a+τ(C18-C13-C14-C15)[10]a
45	1073	1054	1050(m)	ν_s(C6-C5)[13]+ν_a(O23-C2)[12]+ν_a(O25-C6)[10]+φ(C6-C5-C4)[18]a
46	1061	1043		τ(H32-C11-C12-C18)[26]a + τ(H21-C17-C18-C12)[46]
47	1051	1033		νa(C12-C18)[11]+νs(O26-C16)[14]
48	1025	1007		τ(H32-C11-C12-C18)[35]a+τ(H21-C17-C18-C12)[27]+ω(O22-C3-C11-C14)[11]
49	992	976	970(m)	τ(H7-C1-C6-C5)[63] + ω(O23-C1-C3-C2)[15]a ***{Char}***
50	968	951		τ(H8-C4-C5-C6)[16] +τ(H9-C5-C6-C1)[47]+ ω(O25-C1-C5-C6)[10]a
51	864	849		τ(H19-C13-C18-C12)[36]a +τ(H20-C14-C15-C16)[36]
52	948	932	925(w)	ω(O22-C3-C11-C10)[13]a
53	900	885	875(m)	νs(C16-C15)[28]+νs(O27-C15)[12]
54	861	846		φ(O1-C7-C6)[15] + φ(C6-C5-C4)[11]
55	825	811		νs(C6-C5)[21]+φ(C2-C1-C6)[11]a+φ(C6-C5-C4)[21]
56	817	803		τ(C17-C16-C15-C14)[14]a + τ(C18-C13-C14-C15)[15]a +
				ω(O27-C14-C16-C15)[14]a+ω(O26-C15-C17-C16)[10]
57	793	780	780(w)	νa(C6-C5)[12]a
58	769	756		τ(H24-O23-C2-C1)[40]a +ω(O22-C3-C11-C10)[17]a
59	757	744		τ(H24-O23-C2-C1)[50]
60	723	711		τ(H9-C5-C6-C1)[15]a + ω(O25-C1-C5-C6)[31]a+ω(O23-C1-C3-C2)[27]a

Table-II cont..

61	699	687		φ(C3-C10-C11)[10]a
62	675	664	660(w)	ω(O26-C15-C17-C16)[14]a+ω(C12-C13-C17-C18)[17]a
63	646	635	630(w)	νs(C15-C14)[14]+νs(O26-C16)[10]+φ(C17-C16-C15)[11]
64	636	626		φ(C2-C1-C6)[21]
65	615	604	600(msh)	φ(O22-C10-C11)[30]
66	577	567		φ(C2-C1-C6)[13] +φ(O23-C2-C1)[20]
67	532	523		τ(H8-C4-C5-C6)[12] + τ(C6-C5-C4-C3)[33]+
				ω(O25-C1-C5-C6)[14]+ω(O23-C1-C3-C2)[10]a
68	523	514		τ(H20-C14-C15-C16)[13]a + τ(C16-C15-C14-C13)[22]a+
				ω(O27-C14-C16-C15)[17] + ω(O26-C15-C17-C16)[16]a
69	517	508		φ(O23-C2-C1)[22]+φ(O25-C6-C5)[13]
70	483	475		φ(C3-C10-C11)[10]a
71	467	459	450(m)	τ(H29-O26-C16-C15)[83]a+ω(O27-C14-C16-C15)[25] ***{Char}***
72	422	415		τ(C18-C13-C14-C15)[19]a
73	414	407		τ(H28-O25-C6-C1)[93]
74	398	391		νs(C6-C5)[18] +φ(O22-C10-C11)[12]a
75	388	381		φ(C5-C4-C3)[11]+φ(O23-C2-C1)[19]a+φ(O25-C6-C5)[27]
76	357	350		φ(C12-C18-C17)[11]a+φ(O27-C15-C14)[10]+τ(C5-C4-C3-C10)[13]
77	333	327		φ(O26-C16-C17)[20]+φ(O27-C15-C14)[26]
78	316	311		φ(O26-C16-C17)[25]
79	290	285		τ(H30-O27-C15-C14)[17]a+ τ(C17-C16-C15-C14)[12]+
80	274	269		τ(C10-C11-C12-C18)[10]a+ω(O26-C15-C17-C16)[16] τ(H30-O27-C15-C14)[78]a
81	256	252		τ(C2-C1-C6-C5)[48] + τ(C6-C5-C4-C3)[13]a+
				ω(O25-C1-C5-C6)[10] + ω(O23-C1-C3-C2)[24]a
82	231	227		φ(C4-C3-C10)[34] + τ(C17-C16-C15-C14)[14]
83	207	204		τ(C17-C16-C15-C14)[21] +τ(C3-C10-C11-C12)[19]
84	170	167		φ(C3-C10-C11)[17]+φ(C10-C11-C12)[10]+ τ(C3-C10-C11-C12)[15]a
85	139	136		τ(C5-C4-C3-C10)[10] +τ(C3-C10-C11-C12)[36]
86	113	111		φ(C11-C12-C18)[18]a+φ(C12-C18-C17)[19]+ τ(C5-C4-C3-C10)[18]
87	92	91		τ(C5-C4-C3-C10)[18]+τ(C1-C6-C5-C4)[11]a+τ(C4-C3-C10-C11)[18]a
88	42	41		τ(C10-C11-C12-C18)[42]+ω(C12-C13-C17-C18)[13]a
89	37	36		φ(C3-C10-C11)[10]a+φ(C10-C11-C12)[22]a+
				τ(C5-C4-C3-C10)[10]+ τ(C3-C10-C11-C12)[31]
90	6	6		τ(C11-C12-C18-C13)[81]

Abbreviations:

s:-symmetric; a:- antisymmetric; v:-stretching mode;φ:- inplane bendin; τ:- torsional modeg

ω:- out of plane wagging;Char:- characteristic mode

*** *Note:The spectral values of the title compound, has been used from the FT-IR spectrum reported by Manju Bhargavi et.al. al***

Ref:8 https://www.researchgate.net/profile/Manju_Bhargavi12/publication/324269968/figure/fig4/AS:627521703907330@1526624241717 /FT-IR-spectrum-of-a-butein-and-b-butin-IP-in-plane-and-OP-out-ofplane-bends.png".

(O-H) stretch: In vibrational spectra, the strength of hydrogen bond decides the position of O-H band. Generally the *ν*(O-H) stretching vibration appears at 3600-3400 cm^{-1} [21]. In the present study the title molecule showed two weak absorption spikes in FTIR spectra at 3610& 3490 cm^{-1} and for this four vibrational modes are calculated at 3890,3870,3844& 3689 cm^{-1} with 100% PED's.

(C-H) stretch: The aromatic structure rings R1 & R2 of the title compound butein shows the presence of C-H stretching vibration in the region 3280- 3210 cm^{-1} which is the characteristic region for the ready identification of C-H stretching vibration and is assigned with one medium intensity spike obtained at 3350 cm^{-1} and three weak shoulder peaks found at 2950, 2870 and 2810 cm^{-1} in the FTIR spectrum [21]. The C-H modes of deformation such as scissoring, rocking and torsion are obtained below the frequency 1500-1000 cm^{-1} and is very useful for characterization purpose. These C-H modes appears as strong band in FTIR spectrum at 1535 {*characteristic*}, 1240 {*characteristic*}, 1190 & 1050 cm^{-1} are assigned with the calculated frequencies with 1633, 1655, 1484,

1479, 1447, 1437, 1412, 1365,1284, 1243, 1192 and 1054 cm^{-1} . The out-of-plane CH modes of the butein rings are observed at 970 cm^{-1} in the IR spectrum and in the range 976–711cm^{-1} theoretically. These are in accordance with the literature occurring in the region 1000-750 cm^{-1}[22].

(C=O) vibration : Carbonyl absorption is generally found in the spectral region1750-1630 cm^{-1} and the presence of ν(C=O) makes the structure of the title compound fairly rigid whereas the formation of hydrogen bond restricts the disturbance of the charge distribution in the ring and side chains. This is supported by the length of hydrogen bonds provided in the supplementary table T-1. In the present study the ν(C=O) stretching vibration is observed with two very strong spikes at 1670, 1630 cm^{-1} and are assigned to the calculated frequencies 1727and 1716 $cm^{-1}$with high PED values.

***(C-C) Vibration*:** The C-C aromatic stretch known as semicircle stretching gives rise to the characteristic bands in the spectral range of 1600-1000 cm^{-1} [21]. In the present study, C-C vibrational mode is calculated in the range of 1686-885 cm^{-1} and spikes are observed at 1686, 1421, 1412, 1365, 1346, 1298, 1273, 1240,1153,1054 and 885 cm^{-1} in the FTIR spectra. The theoretically calculated φ(C-C-C) in plane bending modes and τ(C-C-C-C) has been found to be consistent with the recorded spectral values.

(C-O) vibration: In the present study, the ν(C-O) stretching vibrational mode is calculated in the frequency range of 1374-1054 cm^{-1}, which coincides well with the experimental values of the FTIR spectra and is supported by the literature [21]. These vibrations are mixed with in plane bending modes of φ(C-C-C) and other vibrational modes, with low PED values.

Lower spectral modes: Lower spectral modes are important because it gives the information about weak intermolecular interactions, which happens in many biological reactions [23]. These modes are very helpful in the interpretation of the effect of electromagnetic radiation on biological systems [24]. In the present study, one torsional mode τ (H7-C1-C6-C5) is calculated at 976 cm^{-1}, mixed with out of plane wagging ω(O23-C1-C3-C2) with 63% and 15% PEDs, and are assigned to 970 cm^{-1} peak in the spectra. This mode seems to be one of the *characteristic* modes of the title compound. The torsional mode τ(H29-O26-C16-C15) with asymmetric vibration is mixed with out of plane wagging ω(O27-C14-C16-C15) with 83% and 25% PEDs in the lower region of spectrum and it also seems to be one of the *characteristic* modes of the title compound. Other lower frequencies are calculated at the values are in the range 415- 6 cm^{-1}as shown in supplementary table T-II.

Electronic Properties

HOMO & LUMO energy orbital participate in chemical reactions or interactions with other species and their energy gap helps, to quantify the chemical reactivity of the molecule [25]. HOMO orbital energy characterizes the ability of electron donating and the LUMO energy characterizes the ability of electron accepting, whereas the HOMO-LUMO energy gap gives the indication about the stability of the compound [26]. Small frontier energy gap clearly indicates that the molecule possesses more polarizability, high chemical reactivity and is termed as *soft molecule* [27, 28]. The 2D plots of HUMO and LUMO are shown in and Figure 3, respectively, and their values are given in Table 1.

Figure 2 of HOMO (-8.47 eV), shows that the entire HOMO is distributed over ring R2 and two oxygen atoms C11 &C12 and has ð bonding character. Fig 3 of LUMO (1.48 eV) shows that most of the LUMO is distributed over ring R2 atoms C10, C11, C12 and ring R2 and maximum charge is transferred on the atoms C10 and then on atoms C11, C12, C18, C17 and C13 in decreasing order. The difference of LUMO and HOMO calculated values gives the value of energy gap which is quite high (9.95 eV) suggesting that butein is less polarizable, bears low chemical reactivity and thus show the characteristics of hard molecule. However butein compounds with metal complexes are reported to be tremendous results as drugs [29]. The MEPS plot mapped on to the iso-electron density surface, simultaneously displays, shape, size and electrostatic potential values of the compound in terms of the color coding and is an important means in the investigation of correlation between molecular structure and the physiochemical property relationship of molecules including bio molecules and drugs [30-35]. The MEPS is also useful in analyzing of one molecule by another, as in drug-receptor and enzyme–substrate interactions [33]. To predict reactive sites for nucleophilic and electrophilic attack for butein the MEPS is calculated. Figure 4 (color scaling -0.067 to +0.067 A.U.) shows that the electron rich regions

reside on the four oxygen atoms O_{22}, O_{23}, O_{26} and O_{27}, are the main binding sites for electrophilic attack for the butein.

Electric Parameters

NLO properties of organic molecules are explained with the help of parameters like dipole moment, polarizability and hyperpolarizability. Polarizability and hyperpolarizability are connected directly to the first and higher order derivatives of the electron density and provide the stability of chemical bonds and characteristics of interactions [37, 38]. The calculated value of dipole moment for butein, is found to be moderate (4.33 Debye) and is attributed due to the presence of highly electron withdrawing carbonyl group (C_{10}=O_{22}).

All the electric parameters are listed in table 1 and it is evident that the component α_{YY} of the mean polarizability <α> has got the highest value (-129e.s.u.), which indicates that the title molecule is elongated maximum along the Y axis as compared to other axes. The total intrinsic hyperpolarizability β_{total} and a component of the first hyper polarizability along the direction of the dipole moment are represented by β.

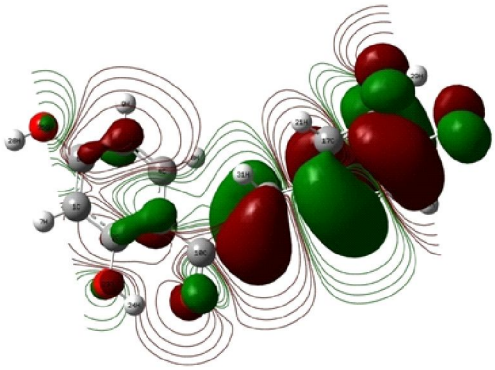

Figure 3 : 2D plot of HOMO of butein as seen by Gaussview 5.0.8 software

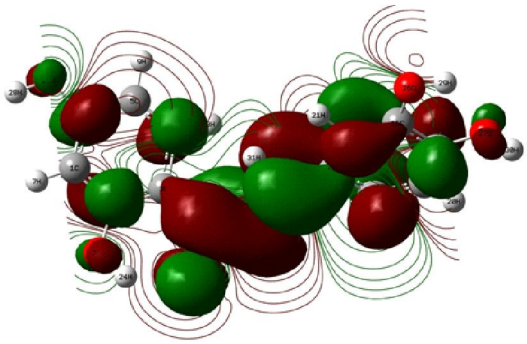

Figure 4 : 2D plot of LUMO of butein as seen by Gaussview 5.0.8 software

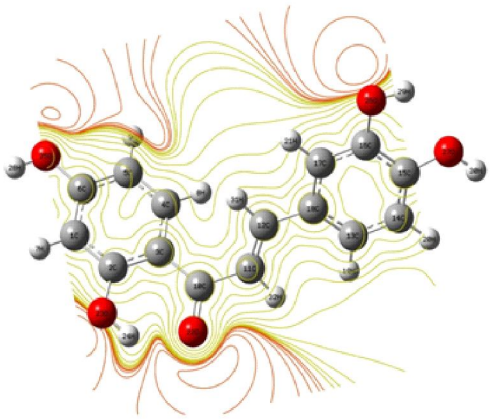

Figure 5 : 2D MEPS plot of butein

Table-1: Electric & Electronic Parameters for Butein Calculated at B3LYP/6-311++G(d,p)

Polarizability	Values	Hyperpolarizability	Values	Parameters	Values
Components	e.s.u.($*10^{-24}$)	Components	e.s.u. ($*10^{-33}$)		
α_{xx}	-85.28	β_{xxx}	116.89	HOMO(eV)	-8.47
α_{xy}	-21.98	β_{XXY}	-4.26	LUMO(eV)	1.48
α_{yy}	-129.21	β_{XYY}	38.80	Band-gap(eV)	9.95
α_{xz}	-10.76	β_{YYY}	4.75		
α_{yz}	5.40	β_{XXZ}	-24.93	Electric Dipole	4.33
α_{zz}	-119.24	β_{XYZ}	-10.24	μ (Debye)	
<α>	**-101.75**	β_{YYZ}	-6.13		
		β_{XZZ}	8.81		
		β_{YZZ}	-0.90		
		β_{ZZZ}	4.33		
		β1	27062.00		
		β2	0.17		
		β3	714.21		
		β_{total}	**166.66**		

The largest component β_{xxx} of hyperpolarizability β_{total} indicates that butein is relatively more optically active along X axis. The β_{total} components are represented in atomic units, where 1 a.u. = 8.3693* 10_{-33} e.s.u. The calculated values of <α> for Butein,

calculated by DFT are -111.75 a.u (or - $0.935*10^{-30}$ e.s.u.) whereas the value of hyperpolarizability β_{total} is 166.66 a.u. (or $1.394 * 10^{-30}$ e.s.u. Urea (β_{total} =0.1947 $*10^{-30}$ e.s.u.) is benchmark compound for NLO properties because it does not have particularly strong nonlinearity, therefore the results are compared with urea. The calculated value of hyperpolarizability of the compound is more than seven times than the hyperpolarizability of urea so it is a good claimant as a NLO material.

Molecular Docking

Molecular docking produces the most reliable measure for assessing the therapeutic value of a given compound. This method explores ways in which two molecules, comprising of a ligand and a receptor fit together and dock to each other. The molecular binding of a ligand to its receptor may alter its function and thus enabling the use of ligand molecule for development of a drug [39]. The target protein has been obtained from Protein Data Bank (PDB) database (PDB ID = 1OG6) [40]. The docking calculations have been performed using Autodock Vina 4.2 [41]. The values of various properties of the enzyme 1OG6 are reported and are as follows; Resolution=2.80Å, R_{free}= 0.238, Clashscore=26, Ramachandran Outliers=1.9% and Sidechain outliers=7% respectively [42]. Ligand-protein interactions like anti-oxidant activities, free radical scavenging activity, apoptotic cell death and protection against oxidative injury in hepatic cells were confirmed using molecular docking analysis. 2D protein-ligand interaction profile image has been created and is presented in figure 6. We have found a strong binding of butein with 1OG6, a protein of an aldo-keto reductase from E.coli complexed with NADPH. It is clear from the figure that butein is docked well with the 1OG6 protein.

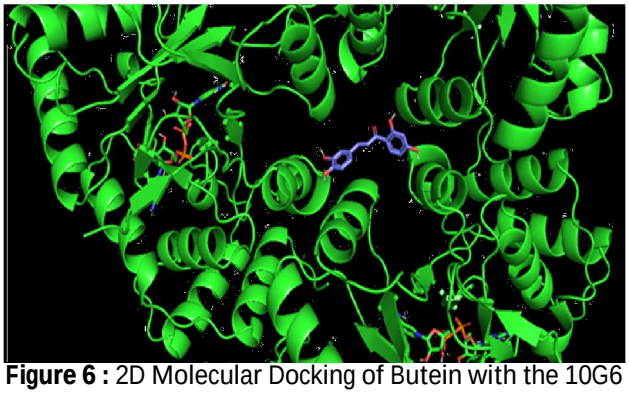

Figure 6 : 2D Molecular Docking of Butein with the 10G6 Protein using Software

CONCLUSION

In this work, we have reported out a comprehensive study on “Butein (2',3,4,4'-Tetrahydroxychalcone)”. The molecular geometry, vibrational wavenumbers and NLO behavior of the title molecule have been calculated using DFT (B3LYP) method adopting 6311++G(d,p) basis set. The nonlinear optical (NLO) behavior of the title molecule has been investigated by the dipole moment, the polarizability and the first hyperpolarizability. The frontier orbital energy gap is calculated as 9.95 eV which suggests that butein is relatively less polarizable, less chemically reactive in itself, bears high kinetic stability and is therefore a comparatively hard molecule. Dipole moment μ, molecular polarizability $<\alpha>$ and total first static hyperpolarizability β_{total} are computed as 4.33 D, -111.75 a.u. and 166.66 a.u. respectively. The β_{total} value is nearly *seven times* compared to that of urea, indicating that butein possesses nonlinear optical properties and is a potential candidate for nonlinear optical applications. The molecular orbitals and MEPS map may lead to the understanding of properties and activity of the compound. The molecular docking study of the butein as ligand with the receptor protein 1OG6 suggests that butein docked well with target protein 1OG6, which indicates that it may be of biological and pharmacological significance. The results of molecular docking study give a strong support to the hypothesis that butein has the potential to emerge as an effective lead candidate for anti-oxidant drug development. However, further in-depth and thorough studies are needed in this direction to validate this prediction. Besides, there is a lot of scope for application of similar molecular docking approaches to corroborate existing hypotheses about the physiological role of butein. Butein also appears to be involved in inhibition of advanced glycation end products which act as reliable markers in Diabetes and Alzheimer’s disease. Further, the effect of butein on activating sertuins which cause NAD-dependent deacetylation of proteins is well documented. We hope that similar molecular docking studies will be aggressively pursued in unraveling the physiological mechanisms of butein and other nutraceuticals.

DECLARATIONS

Funding: Authors did not get any funding from any agency.

Conflicts of interest/Competing interests: Present manuscript does not bear any conflict of interest.

Supplementary Information (SI). Table TI and TII represents the optimized parameters and vibrational assignments respectively and are provided in supplementary data.

REFERENCES

[1] Swamy TK, Yerragunta V, Suman D, Anusha V, Prathima P, Samhitha T (2013) Pyrimidineandits Biologicalactivity: A Review *Pharmatutor*. 1(2): 39-44.

[2(a)] Panche AN, Diwan AD, Chandra SR, (2016) Flavonoids: an overview, J.of Nutritional Sc., vol. 5, e47, page 1-15. doi:10.1017/jns.2016.41(b) Guo P, Chen W, Song J, Cao W, Tian C (2008) A DFT study of the interaction between butein anion and metal cations (M=Mg2+, Cr2+, Fe2+, and Cu2+): Taking an insight into its chelating property.*J. of Mol. Struct.* 849: 33-36.

https://doi:10.1016/j.theochem.2007.10.017.

[3] Cheng ZJ, Kuo SC, Chan SC , Ko FN, Teng CM(1998) Antioxidant properties of butein isolated from Dalbergiaodorifera*, Biochim. etBiophys.Acta.* 1392(2-3): 291-299.

https://doi.org/10.1016/S0005-2760 (98)00043-5

[4] Song NJ, Yoon HJ, Kim KH, Jung SR, Jang WS, Seo CR, Lee YM, Kweon DH, Hong JW, Lee JS, Park KM, Lee KR, Park KW (2013)Butein is a novel anti-adipogenic compound. *J. Lipid Res.* 54:1385-1396.

https://DOI10.1194/jlr.M035576.

[5] Pereira RF, Zhang Z, Park C, Kim D, Kim K, Park Y (2020) Butein inhibits lipogenesis in Caenorhabditiselegans. *BioFactors.*

https://doi.org/10.1002/biof.1667

[6] Wang Y, Chan F, Chen S, Leung LK (2005)The plant polyphenol butein inhibits testosterone- induced proliferation in breast cancer cells expressing aromatase. *Life Sciences*. 77(1):39-51.

https://doi:10.1016/j.lfs.2004.12.014 PMID: 15848217.

[7] Seo WY, Youn GS , Choi SY, Park J (2015) Butein, a tetrahydroxychalcone, suppresses pro-inflammatory responses in HaCaT keratinocytes.*BMB Rep.* 48(9): 495–500. https://doi: 10.5483/BMBRep.2015.48.9.259 PMCID: PMC4641232

[8] Lee EH, Song DG, Lee JY, Pan CH, Um BH, Jung SH (2008) Inhibitory effect of the compounds isolated from Rhusverniciflua on aldose reductase and advanced glycation end products Biol. *Pharm. Bull.* 31 (8): 1626-1630.

https:// doi:10.1248/bpb.31.1626. PMID 18670102.

[9] Frisch MJ, Trucks GW, Schlegel HB et al(2009) Gaussian 09, Revision A.1 Gaussian Inc, , Wallingford CT.

[10] Schlegel HB (1982) Optimization of equilibrium geometries and transition structures. *J Comput. Chem.* 3(2): 214-218.

[11] Petersson DA, Allaham MA (1991) A complete basis set model chemistry. II. Open shell systems and the total energies of the first-row atoms. *J. Chem. Phy.*; 94:6081–90.

[12] Petersson DA, Bennett A, Tensfeldt TG, Allaham MA, Mantzaris WAJ (1988) A complete basis set model chemistry. I. The total energies of closed-shell atoms and hydrides of the first-row elements. *J. Chem.Phys.*; 89:2193–218.

[13] Frisch A et al. Gaussian (2009) *Inc. GaussView*, Version 5.0.8.

[14] Hohenberg P, Kohn W (1964) Inhomogeneous electron gas., *Phys Rev B*. 136: 864-871.

[15] Becke AD (1993) Perspective on "Density functional thermochemistry. III. The role of exact exchange. *J Chem. Phys.* 98: 5648-5652.

[16] Lee C, Yang W, Parr RG (1988) Development of the Colle-Salvetti correlation-energy formula into a functional of the electron density. *Phys. Rev. B*. 37: 785-789.

https://doi.org/10.1103/PhysRevB.37.785

[17] Jamroz MH (2004) Vibrational Energy Distribution Analysis, *VEDA 4 Program*, Warsaw, Poland.

[18](a)Dashing P , Gumpu MB , Thumped P , Rayappan JB B, Ravichandiran V , Pazhani GP, Veerapandian M (2018) *Journal of Photochemistry and Photobiology B*: Biology Volume 182, 122-129.

https://doi.org/10.1002/jcc.540030212

(b) O'Boyle NM, Tenderholt AL and Langner KM. GaussSum *J. Comp. Chem*., 2008, 29, 839-845.

[19] (a) Silverstein RM, Bassler GC, Morrill TC (1991) Spectrometric Identification of Organic Compounds, John Wiley and sons; (b) Socrates G (2001)*Infrared and Raman characteristic Group Frequencies-Tables and Charts*, Third ed. Wiley New York.

[20](a) Karabacak M, Kurt M, Cinar M, Coruh A (2009) Experimental (UV,NMR, IR, and Raman) and theoretical spectroscopic properties of 2-dichoro-6-methylaniline,*Mol.Phys.* 107:253-264 (b) Sundaraganesan N, Ilakiamani S, Saleem H, Wojciechowski PM, MichalskaD (2005) FT-Raman and FT-IR spectra, vibrational assignments and

density functional studies of 5-bromo-2-nitropyridine.*Spectrochim.Acta A Mol and Biomol Spectrosc.* 61(13-14): 2995-3001.

https://doi: 10.1016/j.saa.2004.11.016.

[21] Colthup NB, Daly LH, Wiberley SE (1990) *Introduction to Infrared and Raman Spectroscopy*, Academic Press, New York.

[22] Socrates G (1980) *Infrared Characteristic Group Frequencies*, Wiley-Inter science Publication, New York.

[23] Chou KC (1984) Biological functions of low-frequency vibrations (phonons). III. Helical structures and microenvironment. *Biophys. J.* 45(5): 881-889.

https://doi.org/10.1016/S0006-3495(84)84234-4

[24] Frohlich H (1988) *In Biological Coherence and Response to External Stimuli*: Springer Berlin.

[25] Sklenar H, Jager J (1979) Molecular structure–biological activity relationships on the basis of quantum chemical calculations. *Int. J Quantum Chem*. 16(3): 467-484.

https://doi.org/10.1002/qua.560160306

[26] Fukui K (1982) Role of Frontier Orbitals in Chemical Reactions. *Science.* 218(4574): 747-754.

https://www.jstor.org/stable/1689733

[27] Fleming I (1976) *In Frontier Orbitals and Organic Chemical Reactions*: John Wiley and Sons, New York.

[28] Sajan D, Joseph L, Vijayan N, Karabacak M (2011) Natural bond orbital analysis, electronic structure, non-linear properties and vibrational spectral analysis of L-histidinium bromide monohydrate: a density functional theory; *Spectrochim. Acta A, Mol and Biomol Spectrosc*.81(1): 85-98.

https://DOI: 10.1016/j.saa.2011.05.052

[29] Guo P, Chen W, Song J, Cao W, Tian C (2008)A DFT study of the interaction between butein anion and metal cations (M = Mg2+, Cr2+, Fe2+, and Cu2+): Taking an insight into its chelating property. *Journal of Molecular Structure*. 849(1-3):33-36.

https://doi.org/10.1016/j.theochem.2007.10.017

[30] Murray JS, Sen K (1996), *In Molecular Electrostatic Potentials, Concepts and Applications*: Elsevier Amsterdam.

[31] Alkorta I, Perez JJ (1996) Molecular polarization potential maps of the nucleic acid bases. *Int. J. Quant. Chem.* 57(1): 123- 135.

https://doi.org/10.1002/ (SICI) 1097-461X (1996)57:1%3C123::AID-QUA14%3E3.0.CO;2-9

[32] Scrocco E, Tomasi J (1978), *In Advances in Quantum Chemistry-2 P Lowdin ed*. Academic Press: New York.

[33] Karabacak M, Cinar M (2012)FT-IR, FT-Raman, UV spectra and DFT calculations on monomeric and dimeric structure of 2-amino-5-bromobenzoic acid. *Spectrochim. Acta A Mol and Biomol Spectrosc*. 86: 590-599.

https://doi.org/10.1016/j.saa.2011.11.022

[34] Luque FJ, Orozco M, Bhadane PK, Gadre SR (1993) SCRF calculation of the effect of water on the topology of the molecular electrostatic potential. *J. Phys. Chem*. 97(37): 9380- 9384.

https://doi.org/10.1021/j100139a021

[35] Sponer J, Hobza P (1996) DNA base amino groups and their role in molecular interactions: Ab initio and preliminary density functional theory calculations. *Int. J. Quant. Chem.* 57(5): 959-970.

https://doi.org/10.1002/ (SICI) 1097-461X (1996)57:5%3C959:: AID-QUA16%3E3.0.CO;2-S

[36] Li Y, Liu Y, Wang H, Xiong X, Wei P, Li F(2013) Synthesis, Crystal Structure, Vibration Spectral, and DFT Studies of 4-Aminoantipyrine and Its Derivatives. *Molecules,* 18: 877-893.

https://doi.org/10.3390/molecules18010877

[37] Kleinman DA (1962) Nonlinear Dielectric Polarization in Optical Media. *Phys. Rev. J.*126 (6): 1977- 1979.

https://doi.org/10.1103/PhysRev.126.1977

[38] Pipek J, Mezey PG (1989) A fast intrinsic localization procedure applicable for ab initio and semiempirical linear combination of atomic orbital wave functions. *J. Chem. Phys.* 90(9): 4916- 4926.

https://doi.org/10.1063/1.456588

[39] Srivastava V, Kumar A, Mishra BN, Siddiqui M I (2008) Molecular docking studies on DMDP derivatives as human DHFR inhibitors. *Bioinformation.*3(4):180- 188.

https://dx.doi.org/10.6026%2F97320630003180

[40] <http://www.rcsb.org/pdb/explore.do?structureId=10G6>.

[41] Trott O, Olson A J, *Journal of Computational Chemistry,* 31 (2010)31(2): 455-461.

[42] Williams P A, Cosme J, Ward A, Angove HC, Vinkovic DM, Jhoti H, *Structure of human cytochrome P450 CYP2C9; Full www.PDB X-ray Structure Validation Report.* PDB (2020) https://www.wwpdb.org/validation/2017/XrayValidationReportHelp.
doi: 10.1002/jcc.21334.